

## Parametric autoresonant generation of dark solitons

A. G. Shagalov <sup>\*</sup>

*Institute of Metal Physics, Ekaterinburg 620990, Russian Federation*

L. Friedland <sup>†</sup>

*Hebrew University of Jerusalem, Jerusalem 91904, Israel*



(Received 5 June 2022; accepted 4 August 2022; published 23 August 2022)

The autoresonant generation of dark solitons of the nonlinear Schrödinger (NLS) equation is discussed. The approach is based on capturing the system into a continuing resonance using a small, chirped frequency parametric driving. Adiabatic control of soliton parameters is achieved if the driving amplitude exceeds a threshold.

DOI: [10.1103/PhysRevE.106.024211](https://doi.org/10.1103/PhysRevE.106.024211)

### I. INTRODUCTION

The generation of dark solitons (DS) was first studied in the context of nonlinear optics (see a review in Ref. [1]) and continued attracting attention in the field [2–4]. Similar problems of DS generation were also investigated in applications to Bose-Einstein condensates [5–8] and magnetic materials [9–11].

Methods of generation of DS usually involve large perturbations of the system and do not allow formation of pure solitons with predefined parameters and small remaining perturbations. Typical examples involve phase and density “engineering” [12,13] in Bose-Einstein condensates. In the present work, we propose generation of nearly pure DS by a small amplitude, chirped frequency driving, which allows us to adiabatically control the amplitude of the excited soliton. A similar approach was used previously in excitation of DS by a quasiperiodic field [14] using the effect of autoresonance. The autoresonance is a general phenomenon in nonlinear systems which involves a continuous self-phase-locking of a system to chirped frequency drives [15]. As the driving frequency varies in time, the autoresonant system performs evolution in its parameter space, frequently leading to excitation of nontrivial large amplitude states. This phenomenon was studied in many applications such as planetary dynamics [16], Josephson junctions [17], magnetization dynamics [18], and more. In this paper the DS will be generated by a *parametric* autoresonant driving. A similar approach was applied in Ref. [19] in the context of parametric mode conversion.

The presentation will be as follows. Section II will illustrate parametric autoresonant formation of DS in simulations. Our theoretical analysis of the process will be outlined in Sec. III using the approach developed in Ref. [19] based on Whitham’s averaged variational principle [20].

### II. PARAMETRIC EXCITATION OF DARK SOLITONS IN SIMULATIONS

We consider the parametrically driven nonlinear Schrödinger (NLS) equation

$$i\varphi_\tau + \varphi_{\xi\xi} - (2|\varphi|^2 + \varepsilon \cos \psi)\varphi = 0, \quad (1)$$

where  $\varepsilon \ll 1$  and  $\psi = \varkappa\xi - \int \omega dt$  are the amplitude and the phase of the driving perturbation with constant wave number  $\varkappa$  and slowly varying frequency  $\omega(\tau)$ . If  $\varepsilon = 0$ , Eq. (1) has a simple constant amplitude (homogeneous) solution

$$\varphi = U_0 e^{-2iU_0^2\tau}. \quad (2)$$

A nontrivial solution of Eq. (1) is the well known dark soliton [1] (see the Appendix for details). We shall use Eq. (2) as the initial condition in studying resonant generation and control of DS. In the following, we assume that the driving frequency varies linearly in time,  $\omega(t) = \omega_r - \alpha\tau$ , and crosses the frequency

$$\omega_r = \varkappa\sqrt{\varkappa^2 + 4U_0^2} \quad (3)$$

from above at  $\tau = 0$ . This is the well known *Bogoliubov* resonant frequency [21] for perturbation of the homogeneous state by a small amplitude wave with wave number  $\varkappa$ .

It was shown in [19] that after crossing the resonance the evolution of the driven system may evolve in two different ways. If the driving amplitude is small, the nonlinear shift of the eigenfrequency results in the destruction of the resonance and saturation of the excited wave amplitude at the level of  $O(\sqrt{\varepsilon})$  [22]. However, if the driving amplitude exceeds the threshold [19]

$$\varepsilon_c = \frac{0.82|\alpha|^{3/4}}{U_0(\varkappa^3/\omega_r^3 + 3\varkappa/\omega_r)^{1/2}}, \quad (4)$$

the phase of the excited solution locks to that of the drive and the system remains in resonance for a long time, resulting in excitation of a large amplitude wave. A similar threshold phenomenon with scaling  $\varepsilon_c \sim |\alpha|^{3/4}$  is characteristic of all

<sup>\*</sup>shagalov@imp.uran.ru

<sup>†</sup>lazar@mail.huji.ac.il

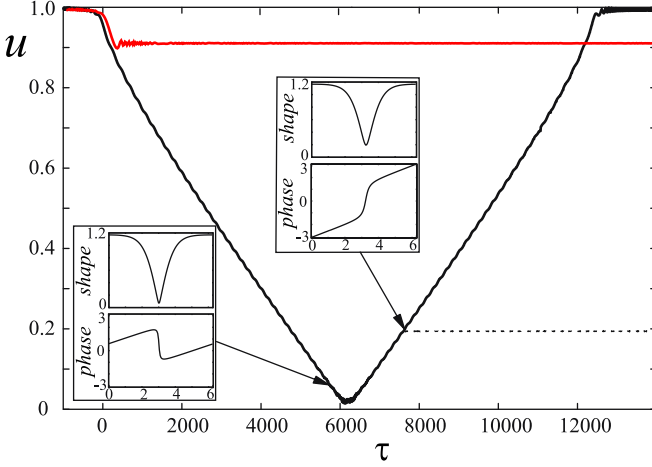


FIG. 1. The autoresonant evolution of the soliton amplitude  $u = \min |\varphi(\xi)|$  (solid line) for  $U_0 = 1$ ,  $\varkappa = 1$ ,  $\alpha = 0.0002$ ,  $\varepsilon = 0.0024 > \varepsilon_c = 0.0012$ . Inner panels show soliton shape  $|\varphi(\xi)|$  and phase  $\arg(\varphi(\xi))$  at  $\tau = 5695$  and  $\tau = 7593$ . The soliton amplitude after switching off the drive at  $\tau = 7594$  is shown by the dashed line. The horizontal red line shows saturation of excitation when  $\varepsilon = 0.00115$  (just below the threshold).

autoresonant chirp-driven systems [15]. This nonlinear bifurcation at  $\varepsilon > \varepsilon_c$  to the continuing phase locking in the system will be used in this paper for generation of DS.

The autoresonant phase-locking means [19]

$$\Delta\Phi = \arg(c_1) - \arg(c_0) - \int \omega d\tau \approx \text{const}, \quad (5)$$

where  $c_{0,1}$  are two coefficients of the Fourier expansion of the solution  $\varphi(\xi, \tau) = \sum c_n(t) \exp(in\varkappa\xi)$ . Figures 1 and 2 show the process of generation of DS in the direct numerical solution of Eq. (1) in the periodic interval  $[0, 2\pi/\varkappa]$ . We start initially from the homogeneous solution (2) and drive the system with the amplitude above the threshold value  $\varepsilon > \varepsilon_c$  (the numerical values of all the parameters in these simulations are given in the figure caption). The horizontal red line in Fig. 1

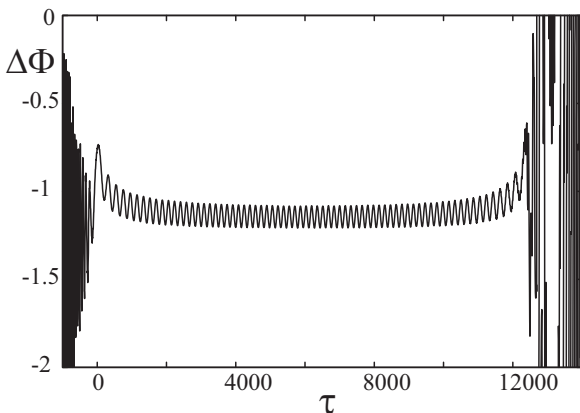


FIG. 2. The phase-locking of the dark soliton with the drive for the same parameters as in Fig. 1. The figure shows the phase difference  $\Delta\Phi(\tau)$  [see Eq. (5)].

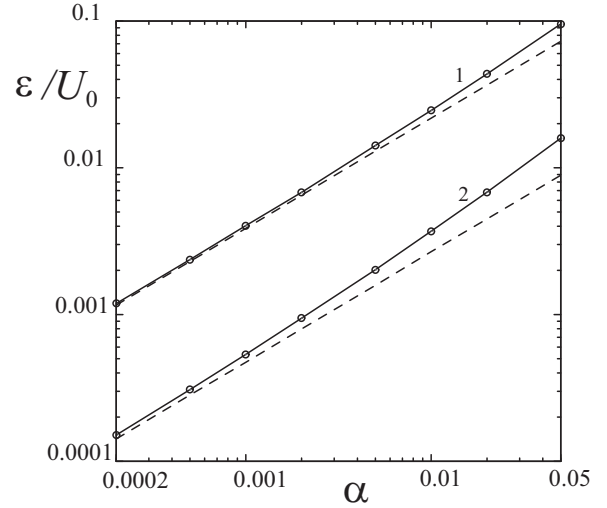


FIG. 3. The threshold on the driving amplitude  $\varepsilon$  vs the driving frequency chirp rate  $\alpha$ . The solid lines show the numerical results for  $U_0 = 1$  (line 1) and  $U_0 = 4$  (line 2) for  $\varkappa = 1$ . The dotted lines are the theoretical thresholds [Eq. (4)].

illustrates saturation of excitation just below the threshold ( $\varepsilon = 0.96\varepsilon_c$ ).

We define the amplitude of the excited “dark” wave as  $u = \min |\varphi(x)|$ . At the initial stage, the amplitude of the uniform solution is weakly perturbed (see Fig. 1), but after crossing the resonance at  $\tau = 0$ , it decreases rapidly. At this stage, the autoresonant phase locking in the system is observed as illustrated in Fig. 2. With the decrease of the amplitude  $u$ , the evolution yields a DS, which is seen in the left inner panel of Fig. 1, where the soliton shape  $|\varphi(\xi)|$  and phase  $\arg[\varphi(\xi)]$  are shown. At  $\tau \approx 6200$  the soliton has amplitude close to zero. Later the amplitude increases, while the soliton changes its phase structure as is seen in the right internal panel of Fig. 1 at  $\tau = 7593$ . Finally, the amplitude increases approaching the initial homogeneous value and the phase-locking is destroyed. We have also found that, if the driving perturbation is switched off at any time of the process, the solution conserves its shape and phase structure, demonstrating the stability of the excited solution. This result is illustrated in Fig. 1 by the dotted line after switching off the drive at  $\tau = 7594$ . Thus, our approach allows one to generate free DS with arbitrary amplitudes.

Figure 3 shows the comparison of the numerically found threshold of autoresonance with the theoretical formula (4). It demonstrates a very good agreement in a smaller amplitude limit.

Our simulation also showed that far from the soliton core the excited solution has the simple asymptotic form  $\varphi \rightarrow U \exp\{iK\xi\}$ . We have calculated the time evolution of  $K(\tau)$  in the process of DS generation, and show this evolution in Fig. 4. In the initial stage, (2) is a uniform wave with  $K = 0$ . In the intermediate stage, when the DS with  $u \approx 0$  is formed, the wave number  $K$  approaches  $\varkappa/2$  and in the final stage of excitation the wave regains the same initial constant amplitude  $|\varphi| \approx U_0$ , but with a different wave number  $K \approx \varkappa$ . This process was described in Ref. [19] as mode conversion of the flat wave from one wave number to another, and no

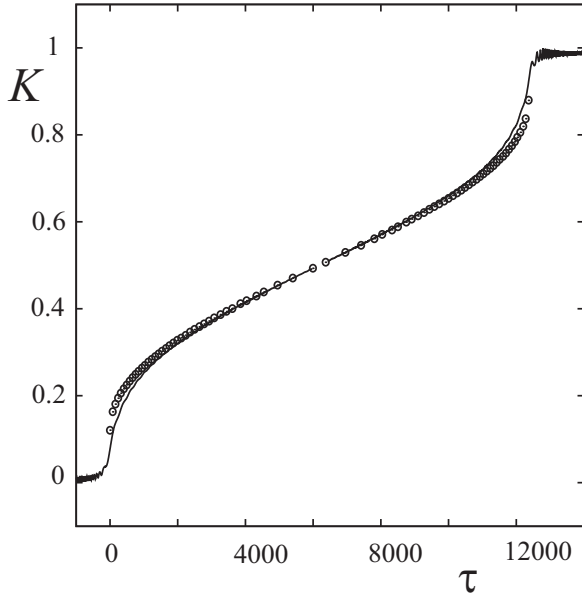


FIG. 4. The autoresonant dark soliton wave number  $K(t)$  in the soliton tail (full line) for parameters of Fig. 1. The theoretical prediction [see Eq. (13) in the next section] is shown by open circles.

conversion was observed if  $\epsilon < \epsilon_c$ . Now we have seen that above the threshold this transformation occurs via excitation of the dark solitons in the process of evolution.

Finally, we have compared the velocity of the numerically excited solutions with the theoretical velocity of dark solitons [see Eq. (A4) in the Appendix] and show this comparison in Fig. 5. We observe good agreement except at the initial and final transient stages. On the other hand, the linearly decreasing soliton velocity coincides with the phase velocity of driving wave  $v_p = \omega(\tau)/\varkappa$ , yielding another illustration of autoresonant phase synchronization between the soliton and the driving perturbation. A variational theory explaining all these numerical results on parametric autoresonance in the NLS system will be discussed next.

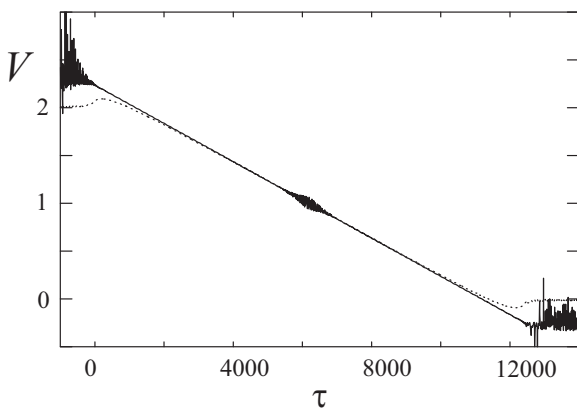


FIG. 5. The velocity  $V(\tau)$  of the autoresonant soliton for parameters of Fig. 1 in numerical simulations (solid line) and from Eq. (A4) in the Appendix (dotted line)

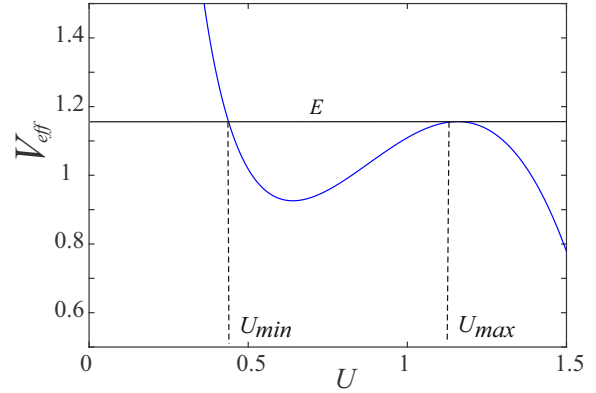


FIG. 6. The effective potential  $V_{\text{eff}}$  versus  $U$ .

### III. VARIATIONAL ANALYSIS OF PARAMETRICALLY DRIVEN CHIRPED DARK SOLITONS

The theoretical approach developed in [19] is based on Whitham's variational principle [20] and allows a full description of parametric autoresonant excitation of NLS solutions. This theory describes two timescale solutions of Eq. (1) of the form  $\varphi(\xi, \tau) = U e^{i\theta}$ , with  $U = U(\Theta, \tau)$  and  $\theta = -\int \Omega_0(\tau) d\tau + V(\Theta, \tau)$ , where  $\Theta = \varkappa\xi - \int \Omega(\tau) d\tau$  is the fast variable, while  $\Omega$  and  $\Omega_0$  are slow parameters. Remarkably, to a good approximation, the NLS solution can be viewed as a slowly evolving state in the *undriven* problem by making a *single* assumption that the slowly varying driving frequency  $\omega(\tau)$  of the parametric drive and  $\Omega(\tau)$  are continuously locked after passage through the linear resonance in the problem. The same theory also showed that this autoresonant phase locking is stable if the driving amplitude exceeds threshold (4), while the exact driven NLS solution performs small oscillations around the above mentioned undriven quasisteady state. In contrast to Ref. [19] focused on studying the process of complete autoresonant mode conversion from a uniform NLS solution into a traveling wave, in this section we neglect the driving and use the assumption  $\omega(\tau) = \Omega(\tau)$  to find the autoresonant dark soliton parameters and soliton shape. The autoresonant quasisteady state dynamics is described by the spatial evolution of a quasiparticle in an effective potential [19], i.e.,

$$U_{\xi\xi} = -\partial V_{\text{eff}}/\partial U, \quad (6)$$

where

$$V_{\text{eff}} = \frac{B^2}{2U^2} + \frac{R}{2}U^2 - \frac{1}{2}U^4 \quad (7)$$

and  $B^2$  and  $R = \Omega_0 + \frac{1}{4}(\Omega/\varkappa)^2$  are slow time dependent parameters. This potential is illustrated in Fig. 6, where the horizontal line shows the energy  $E(\tau)$  of the quasiparticle at some time. It was also shown in Ref. [19] that assuming  $\Omega = \omega(\tau)$  the remaining three slow parameters in the problem,  $B$ ,  $R$ , and  $E$  can be found numerically at each time by

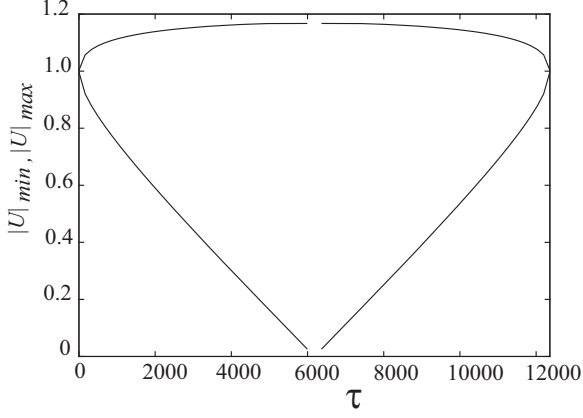


FIG. 7. Maxima and minima of the autoresonant NLS solution versus time for parameters of Fig. 1.

solving three algebraic equations

$$\frac{\partial J}{\partial A} = \frac{1}{\varkappa}, \quad (8)$$

$$\frac{\partial J}{\partial B} = \frac{\Omega}{2\varkappa^2}, \quad (9)$$

$$\frac{\partial J}{\partial R} = -\frac{U_0^2}{2\varkappa} \quad (10)$$

involving the action integral

$$J(A, B, R) = \frac{1}{2\pi} \oint \sqrt{2[E - V_{\text{eff}}(B, R, U)]} dU \quad (11)$$

of the quasiparticle with integration over a closed trajectory at a given energy  $E$ . Note that Eq. (8) states that the spatial period of oscillations of  $U$  in the quasipotential should be that of the driving field,  $2\pi/\varkappa$ . When all the slow parameters are known, the solution of  $U(\xi)$  at each time is given by integration:

$$\int_{U_{\min}}^U \frac{dU'}{\sqrt{2[E - V_{\text{eff}}(B, R, U)]}} = \xi - \xi_{\min}; \quad (12)$$

see Fig. 1 for the definition of  $\xi_{\min}$  and  $U_{\min}$ . The case of  $\varkappa \rightarrow 0$ , i.e., when  $E$  equals the local maximum of  $V_{\text{eff}}$ , corresponds to the soliton solution (see Appendix), and when  $\varkappa$  is sufficiently small we are close to the soliton solution. This is the case of the numerical simulations in Sec. II for  $U_0 = 1$ ,  $\varkappa = 1$ ,  $\alpha = 0.0002$  as we demonstrate below. We have solved the quasisteady state problem in this example as describe above and show the maxima and minima of  $U$  versus time in Fig. 7. Let us assume that  $\varkappa = 1$  is sufficiently small and this solution can be approximated by the soliton solution [see Eqs. (A2)–(A4) in the Appendix] We have found in the simulations described in Sec. II that in the driven problem the condition  $v \approx \omega(\tau)/\varkappa$  is consistent with the autoresonant phase-locking assumption. Under this condition [see Eq. (A4)]

$$K = U_{\min} + \frac{\omega(\tau)}{2\varkappa}. \quad (13)$$

At this stage, we identify  $U_{\min}$  and  $U_{\max}$  in the soliton formulas (A2)–(A4) with those in Fig. 7 and show the resulting  $K$  versus time by open circles in Fig. 4, showing a good

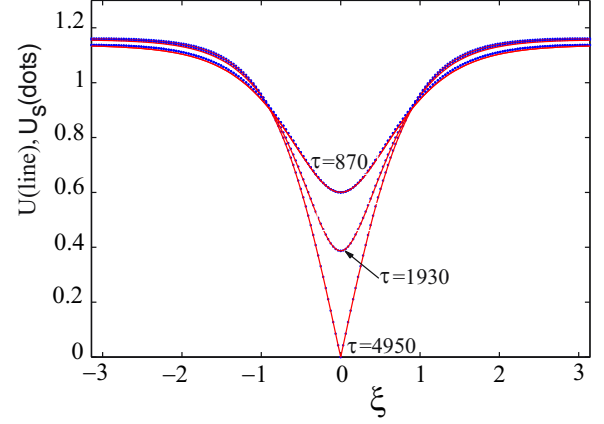


FIG. 8. The shapes of the autoresonant solutions in Fig. 7 from the variational theory at three different times  $\tau = 870, 1930, 4950$  of evolution (solid lines) and the corresponding shapes from the dark soliton formula (A2) (dotted lines).

agreement with simulations (full line in Fig. 4) except near the linear resonance points. We have also calculated the spatial form of  $U$  at three times  $\tau = 870, 1930, 4950$  using Eq. (12) and compared these results with the soliton solution (A2) in Fig. 8. The agreement is excellent, showing that  $\varkappa = 1$  in this example can be viewed as small. However, when the calculation is repeated for  $\varkappa = 2$  (see Fig. 9), larger deviations from the pure soliton solution at the tails can be observed.

#### IV. CONCLUSIONS

This study demonstrates that the parametric autoresonance in the driven NLS equation comprises a promising approach to generate nearly pure DS in condensed matter. In autoresonance, a persistent stable phase-locking of the soliton to a chirped frequency wavelike drive is established. The effect takes place when the driving amplitude exceeds the threshold value [Eq. (4)] scaling with the driving frequency chirp rate as  $\alpha^{3/4}$  after the frequency passes the Bogoliubov resonance.

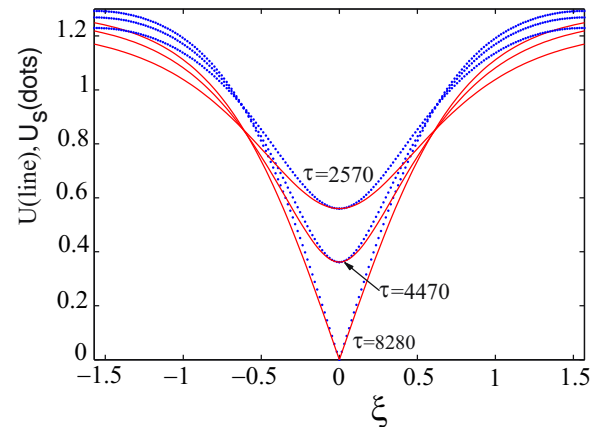


FIG. 9. The shapes of the autoresonant solutions from the variational theory at three different times  $\tau = 870, 1930, 4950$  of evolution (solid lines) and the corresponding shapes from the dark soliton formula (A2) (dotted lines). The parameters are the same as in Fig. 8, but  $\varkappa = 2$  instead of  $\varkappa = 1$ .

Slow variation of driving frequency allows to adiabatically control the amplitude and velocity of the excited DS for a long time. If the driving perturbation is switched off at some time during the autoresonant evolution, we are left with a stable free DS. Thus, the method provides management of large amplitude solitons by a small amplitude driving. We applied the Whitham's averaged variational approach in studying autoresonant NLS solutions [19] to show that the parametrically driven autoresonant DS solutions can be fully described via the motion of a quasiparticle in an effective potential. Furthermore, a single assumption of a continuous resonance in the driven system allows one to calculate the parameters and shape of the excited solution by solving a set of three algebraic equations, (8)–(10), involving the action integral of the oscillating quasiparticle. We showed an excellent agreement of this theory with simulations and that in the case of sufficiently small wave number of the driving wave the autoresonant solution assumes nearly pure DS shape. In addition to the soliton, the NLS equation has other solutions. For example, multiphase waves comprise a class of such solutions [23] and are represented by nonlinear functions  $\varphi = \varphi(\theta_1, \theta_2, \dots)$  of several phase variables  $\theta_i = k_i \xi - \omega_i \tau$ . These waves were autoresonantly excited previously via a direct driving [24], and studying a similar process using parametric driving is an interesting goal for the future. Finally, we also expect applicability of the autoresonant approach to other generalized NLS (GNLS) equations provided the existence of resonances in the system and sufficiently small dissipation. The open problem in this case would be the existence of the threshold [similar to Eq. (4)], which will depend on the structure of the GNLS.

#### ACKNOWLEDGMENTS

This work is supported by the US-Israel Binational Science Foundation Grant No. 2020233.

#### APPENDIX: DARK SOLITONS

We rewrite the DS solution [1] in the form including the soliton phase,

$$\varphi_s(x, t) = U_s e^{i(\Psi + \Psi_N)}, \quad (\text{A1})$$

where the soliton shape and velocity are

$$U_s = U_{\max} \sqrt{1 - \frac{a^2}{\cosh^2[aU_{\max}(\xi - v\tau)]}} \quad (\text{A2})$$

with  $U_{\max}$  and  $U_{\min}$  being the maximum and minimum values of the solution, while parameter  $a$  ( $0 < a < 1$ ) is

$$a = \sqrt{1 - \left(\frac{U_{\min}}{U_{\max}}\right)^2}. \quad (\text{A3})$$

The soliton velocity is

$$v = 2(K - U_{\min}), \quad (\text{A4})$$

and its phase includes

$$\Psi = -(K^2 + 2U_{\max}^2)\tau + K\xi, \quad (\text{A5})$$

$$\Psi_N = -\tan^{-1}\{\mu \tanh[aU_{\max}(\xi - v\tau)]\}. \quad (\text{A6})$$

where  $\mu = \sigma a / \sqrt{1 - a^2}$  and parameter  $\sigma \pm 1$  defines the sign of the nonlinear shift of soliton phase  $\Psi_N(-\infty) - \Psi_N(+\infty)$ . The soliton velocity is

$$v = 2(K - \sigma U_{\min}). \quad (\text{A7})$$

The soliton is located at the point  $x_0 = v\tau$ , where its shape is at its minimum value  $U_{\min}$  and as  $\xi \rightarrow \pm\infty$  the shape approaches its maximum value  $U_{\max}$ . The case of  $a \rightarrow 1$  corresponds to the “pure” DS with the amplitude equal to zero, in contrast to a “gray” soliton with  $a < 1$  and the amplitude greater than zero.

- 
- [1] Y. S. Kivshar and B. Luther-Davies, *Phys. Rep.* **298**, 81 (1998).
- [2] G. Shao, Y. Song, J. Guo, J. Zhao, D. Shen, and D. Tang, *Opt. Express* **23**, 28430 (2015).
- [3] S. Yang, Q.-Y. Zhang, L. Li, L. Jen, and S.-C. Chen, *Infrared Phys. Tech.* **121**, 104043 (2022).
- [4] N. Jhajj, I. Larkin, E. W. Rosenthal, S. Zahedpour, J. K. Wahlstrand, and H. M. Milchberg, *Phys. Rev. X* **6**, 031037 (2016).
- [5] A. Romero-Ros, G. C. Katsimiga, P. G. Kevrekidis, B. Prinari, G. Biondini, and P. Schmelcher, *Phys. Rev. A* **103**, 023329 (2021).
- [6] V. A. Brazhnyi and A. M. Kamchatnov, *Phys. Rev. A* **68**, 043614 (2003).
- [7] C. Wang, P. G. Kevrekidis, T. P. Horikis, and D. J. Frantzeskakis, *Phys. Lett. A* **374**, 3863 (2010).
- [8] G. Verma, U. D. Rapol, and R. Nath, *Phys. Rev. A* **95**, 043618 (2017).
- [9] W. Tong, M. Wu, L. D. Carr, and B. A. Kalinikos, *Phys. Rev. Lett.* **104**, 037207 (2010).
- [10] M. M. Scott, M. P. Kostylev, B. A. Kalinikos, and C. E. Patton, *Phys. Rev. B* **71**, 174440 (2005).
- [11] M. Wu, B. A. Kalinikos, and C. E. Patton, *Phys. Rev. Lett.* **93**, 157207 (2004).
- [12] Z. Dutton, M. Budde, C. Slowe, and L. V. Hau, *Science* **293**, 663 (2001).
- [13] J. Denschlag, J. E. Simsarian, D. L. Feder, C. W. Clark, L. A. Collins, J. Cubizolles, L. Deng, E. W. Hagley, K. Helmerson, W. P. Reinhardt, S. L. Rolston, B. I. Schneider, and W. D. Phillips, *Science* **287**, 97 (2000).
- [14] M. A. Borich, A. G. Shagalov, and L. Friedland, *Phys. Rev. E* **91**, 012913 (2015).

- [15] L. Friedland, *Scholarpedia* **4**, 5473 (2009).
- [16] L. Friedland, *Astrophys. J. Lett.* **547**, L75 (2001).
- [17] K. W. Murch, R. Vijay, I. Barth, O. Naaman, J. Aumentado, L. Friedland, and I. Siddiqi, *Nat. Phys.* **7**, 105 (2011).
- [18] G. Klughertz, P-A. Hervieux, and G. Manfredi, *J. Phys. D* **47**, 345004 (2014).
- [19] L. Friedland and A. G. Shagalov, *Phys. Rev. E* **94**, 042216 (2016).
- [20] G. B. Whitham, *Linear and Nonlinear Waves* (Wiley, New York, 1974).
- [21] A. J. Leggett, *Rev. Mod. Phys.* **73**, 307 (2001).
- [22] R. Z. Sagdeev, D. A. Usicov, and G. M. Zaslavsky, *Nonlinear Physics* (Harwood Academic, Reading, UK, 1988).
- [23] G. Y. Ma and M. J. Ablowitz, *Stud. Appl. Math.* **65**, 113 (1981).
- [24] L. Friedland and A. G. Shagalov, *Phys. Rev. E* **71**, 036206 (2005).